Numerical Computation of Hansen-like Expansions

Sergei A. Klioner
Lohrmann Observatorium, Mommsenstr. 13, 01062 Dresden, Germany *

Akmal A. Vakhidov and Nickolay N. Vasiliev
Institute of Theoretical Astronomy, nab.Kutuzova, 10, St.Petersburg, 191187, Russia

Submitted on 20 March 1997 to *Celestial Mechanics and Dynamical Astronomy*

Abstract. Fourier expansions of elliptic motion functions in multiples of the true, eccentric, elliptic and mean anomalies are computed numerically by means of the fast Fourier transform. Both Hansen-like coefficients and their derivatives with respect to eccentricity of the orbit are considered. General behavior of the coefficients and the efficiency (compactness) of the expansions are investigated for various values of eccentricity of the orbit.

Key words: elliptic motion, Hansen coefficients, satellite motion.

1. Introduction

When constructing analytical and semi-analytical theories of motion of artificial Earth satellites and other celestial bodies we face the problem to expand some functions of coordinates into trigonometric series with the coefficients depending on the eccentricity of the orbit. Numerical efficiency of such series and, therefore, the quality of the resulting theory of motion depends substantially not only on the eccentricity of the orbit but also on the angular variable in multiples of which the expansions are constructed. True, eccentric or mean anomalies are usually used as the trigonometric argument of these expansions. A few years ago it was suggested to use trigonometric expansions in multiples of a new independent variable called elliptic anomaly (Brumberg, 1992; Brumberg and Fukushima, 1994). Preliminary studies showed (Brumberg and Fukushima, 1994) that the series in multiples of the elliptic anomaly in many cases converge faster than the series in multiples of any classical anomaly. It allows one to use the elliptic anomaly very efficiently for constructing theories of motion of celestial bodies (see, for example, Vasiliev, Vakhidov and Sokolsky, 1996; Vakhidov and Vasiliev, 1996). On the other hand, no sufficiently detailed study of the question, which anomaly is more effective for computing various kinds of perturbations in motion of celestial bodies for different values of eccentricity, has been yet performed.

* on leave from Institute of Applied Astronomy, 197042, St.Petersburg, Russia

In this paper we propose an effective algorithm of numerical computation of Hansen-like coefficients corresponding to various anomalies as well as the derivatives of these coefficients with respect to the eccentricity. The algorithm is based on the fast Fourier transform (FFT) and enables us to compute at once all the Fourier coefficients of a given function, absolute value of which is higher than a given limit. The analogous ideas to use the fast Fourier transform to compute numerically the special functions appearing in celestial mechanics have been proposed, e.g., by Goad (1987). However, our algorithm has the advantage of keeping track automatically of all kinds of errors of computations. Making use of our algorithm we investigate numerically how fast the coefficients of trigonometric series in multiples of different anomalies decrease for various values of the eccentricity. In particular, one of the important problems for practice is to study numerical efficiency of various expansions of the satellite perturbing function both for the perturbations due to oblateness of the central body and for the perturbations from external bodies. An attempt to consider this problem was done already by Brumberg and Fukushima (1994), but, since the authors considered only a few first terms of the expansion, the results presented in that paper are not detailed enough to provide a definitive answer for practice.

In the present paper we study trigonometric expansions in multiples of four different anomalies: true, eccentric, mean and elliptic. It is clear that our approach could be easily used also for computing the expansions in multiples of any other angular variable (e.g., for the anomalies introduced in (Bond and Janin, 1981; Ferrandiz *et al.*, 1987)).

Let us stress that the aim of our research is not to obtain analytical estimations connected with the convergence of trigonometric series under consideration, but to study the qualitative behavior of the Fourier coefficients of elliptic motion functions on the basis of numerical experiments.

2. Hansen-like Coefficients and Their Computation

We consider the following expansion

$$\left(\frac{r}{a}\right)^n \exp\left(\overset{\circ}{\imath}\, mv\right) = \sum_{s=-\infty}^{\infty} X_s^{n,m}(e) \exp\left(\overset{\circ}{\imath}\, sx\right), \tag{1}$$

where r, v are the radius-vector and the true anomaly, respectively, defining the position of a body on an elliptic orbit, a is the semi-major axis of the orbit, n, m are integers, x corresponds to one of the above mentioned anomalies, $\overset{\circ}{\imath}$ is the imaginary unit. The coefficients $X_s^{n,m}$

depend on the eccentricity e of the orbit. Expansion (1) is widely used in practical celestial mechanics (for example, for constructing analytical and semi-analytical theories of satellite motion). The aim of our research is to study the behavior of the coefficients $X_s^{n,m}$ for various anomalies and various values of the eccentricity.

In order to compute $X_s^{n,m}$ we use a special approach based on the fast Fourier transform. This approach is very convenient to solve our problem from several points of view. First, numerical Fourier analysis with the FFT is very efficient for computing Fourier expansion of a function which can be computed numerically. In celestial mechanics such an approach has been used, for example, in (Chapront and Simon, 1996; Brumberg and Klioner, 1995; Klioner, 1997) and has shown its high efficiency. Second, the technique based on the fast Fourier transform may be easily applied to any anomaly x, in multiples of which the expansion of coordinates is constructed. Third, this approach can be identically applied for any values of the eccentricity $e \in [0, 1[$ including those very close to 1. Moreover, we obtain simultaneously all the coefficients $X_s^{n,m}$ for fixed n and m from a given interval of values for the index s and/or all the coefficients $X_s^{n,m}$, magnitudes of which are larger than a given limit.

For all anomalies we use the following computational scheme for the coefficients $X_s^{n,m}(e)$.

1. For a fixed value of the eccentricity e we compute the values of the true anomaly v for 2^N values of x distributed uniformly in the interval $[0, 2\pi[$: $x_i = 2\pi/2^N \times (i-1)$, $i = 1, 2, \ldots, 2^N$. At this step of the algorithm we solve (numerically) the equation $v = v(x)$.

2. For all 2^N values of v and for the given n and m we evaluate the left-hand side of (1).

3. By means of the fast Fourier transform we compute the numerical values of the coefficients $\tilde{X}_s^{n,m}$ satisfying in each from 2^N points $x = x_i$ the following relation

$$\left(\frac{r}{a}\right)^n \exp\left(\overset{\circ}{\imath}\, mv\right) = \sum_{s=1-2^{N-1}}^{2^{N-1}} \tilde{X}_s^{n,m}(e) \exp\left(\overset{\circ}{\imath}\, sx\right). \qquad (2)$$

The coefficients $\tilde{X}_s^{n,m}$ differ from the true values of the Fourier coefficients $X_s^{n,m}$ because of errors of aliasing (see, e.g., Press *et al.*, 1992) and numerical round-off errors. The latter source of errors can be tackled by using the fact that $X_s^{n,m}$ are real functions of the eccentricity. Therefore evaluating the Fourier coefficients in complex form (i.e., by

a standard complex FFT procedure) we can use the imaginary parts of the obtained coefficients to estimate the numerical round-off errors of computations. In particular, we find the maximal (in absolute value) imaginary part $\Im$ among all the coefficients computed by means of the FFT and retain only those coefficients, the real part of which is sufficiently larger than $\Im$. As additional test of the algorithm, we make the inverse fast Fourier transform with the retained coefficients and find the difference between the initial and restored functions. This difference allows us to check the overall accuracy of our computations. In order to make errors of aliasing negligible we always check that the coefficients retained after accounting for the numerical round-off errors are sufficiently far from the boundaries of the interval $s \in [1-2^{N-1}, 2^{N-1}]$. If it is not the case we increase the value of N by 1 and repeat the computations.

For each kind of computations (including those of the derivatives of the Hansen-like coefficients described in Section 3 below) we check that our results coincide with the results computed by means of other known methods within expected numerical errors. It is sufficient to check this for a low value of the eccentricity. For a larger value (for example, $e = 0.9$) the use of other methods becomes very difficult or even impossible.

Let us briefly discuss how to solve the equation $v = v(x)$ for each anomaly.

2.1. True Anomaly

In this case we do not need to solve the equation $v = v(x)$. We can simply tabulate the left-hand side of the equation

$$\left(\frac{r}{a}\right)^n \exp\left(\overset{\circ}{\imath}\, mv\right) = \sum_{s=-\infty}^{\infty} V_s^{n,m}(e) \exp\left(\overset{\circ}{\imath}\, sv\right) \tag{3}$$

in the points distributed uniformly with respect to v.

2.2. Eccentric Anomaly

In order to compute the coefficients of the expansions in multiples of the eccentric anomaly g

$$\left(\frac{r}{a}\right)^n \exp\left(\overset{\circ}{\imath}\, mv\right) = \sum_{s=-\infty}^{\infty} G_s^{n,m}(e) \exp\left(\overset{\circ}{\imath}\, sg\right) \tag{4}$$

we evaluate the left-hand side of (4) in the points distributed uniformly with respect to g. The values of the true anomaly are calculated in these points by means of the well-known relation

$$\tan\frac{v}{2}=\sqrt{\frac{1+e}{1-e}}\tan\frac{g}{2}. \tag{5}$$

2.3. Mean Anomaly

For the expansions in multiples of the mean anomaly l

$$\left(\frac{r}{a}\right)^n \exp\left(\overset{\circ}{1}\, mv\right)=\sum_{s=-\infty}^{\infty} L_s^{n,m}(e)\exp\left(\overset{\circ}{1}\, sl\right) \tag{6}$$

we need to compute the values of the true anomaly in the points distributed uniformly with respect to l. To this end we have to solve in these points the Kepler equation

$$l=g-e\sin g \tag{7}$$

enabling one to find the numerical values of the eccentric anomaly g and by using (5) the corresponding values of the true anomaly v.

In case of highly eccentric orbits it is not efficient to solve (7) by means of the classical iteration method or the method of Newton iterations because of slow convergence of the iteration process. It is more reasonable to use in that case special methods of solving the Kepler equation (see, for example, Danby and Burkardt, 1983).

2.4. Elliptic Anomaly

According to (Brumberg, 1992) the elliptic anomaly w is defined as

$$w=\frac{\pi}{2}\left(\frac{F\left(g+\frac{\pi}{2},e\right)}{K(e)}-1\right), \tag{8}$$

where F is the elliptic integral of the first kind, K is the complete elliptic integral of the first kind. In order to compute the coefficients of the expansion in multiples of the elliptic anomaly

$$\left(\frac{r}{a}\right)^n \exp\left(\overset{\circ}{1}\, mv\right)=\sum_{s=-\infty}^{\infty} W_s^{n,m}(e)\exp\left(\overset{\circ}{1}\, sw\right), \tag{9}$$

we have to evaluate the true anomaly in the points distributed uniformly with respect to w. It can be done using the inverse of (8)

$$g=\operatorname{am}\left(K(e)\left(\frac{2w}{\pi}+1\right),e\right)-\frac{\pi}{2} \tag{10}$$

and computing K and the elliptic amplitude $\mathrm{am}(x, e)$ numerically. Alternatively one can use the Fourier expansion of (10) (Brumberg, 1992)

$$g = w + 2\sum_{s=1}^{\infty} \frac{(-1)^s}{s} \frac{q^s}{1+q^{2s}} \sin 2sw, \tag{11}$$

where q is the nome

$$q = \exp\left(-\pi \frac{K\left(\sqrt{1-e^2}\right)}{K(e)}\right). \tag{12}$$

This expansion is known to converge quite rapidly even for large eccentricities due to relatively small value of q. Eq. (5) is again used to compute the corresponding values of v.

2.5. Numerical Results

We designed a package of computer programs in Maple (Char *et al.*, 1993) which allows one to evaluate the coefficients of expansions (3), (4), (6) and (9) for any given values of the indices n and m and any eccentricity $e \in [0, 1[$. Arbitrary-precision arithmetic implemented in Maple is used herewith. The option to change numerical precision of computations is quite useful for the investigation of both our numerical technique and the expansions themselves. Actually we do not use any specific Maple features and it is quite easy to re-write the programs into any effective computer language (e.g., FORTRAN) to speed up the calculations further. For given m, n and e our software computes automatically all the coefficients which could be reliably computed using the given precision of arithmetic. The package automatically accounts for both numerical round-off errors and errors of aliasing along the lines described above. A more detailed discussion of the package can be found in (Vasiliev, Vakhidov and Klioner, 1996; Klioner *et al.*, 1996).

We calculated trigonometric expansions (3), (4), (6) and (9) for several dozens pairs of the indices n and m which appear, e.g., in the expansions of the satellite perturbing function and for four representative values of the eccentricity 0.1, 0.5, 0.75, 0.9. Principal features of the behavior of the coefficients $X_s^{n,m}$ are described below.

2.5.1. *Case* $n < 0$

The expansions with $n < 0$ are used when considering, e.g., perturbations due to oblateness of the central body. Our numerical experiments for $n < 0$ show that the anomalies can be ordered according to the compactness of the corresponding trigonometric series as follows: true (most

compact series), elliptic, eccentric, mean (least compact series). Indeed, for $n < 0$ expansion (3) in multiples of the true anomaly reduces to a finite polynomial. Moreover, the coefficients $V_s^{n,m}(e)$ decrease faster than the coefficients of expansions in multiples of other anomalies. On Figures 1–4 we see typical cases of the behavior of the coefficients $V_s^{n,m}(e)$, $G_s^{n,m}(e)$, $L_s^{n,m}(e)$, $W_s^{n,m}(e)$ of expansions (3), (4), (6) and (9).

Our calculations show that 1) the faster the series in multiples of a given anomaly converge, the larger is the maximal coefficient of the corresponding series, and the smaller is the value of s for this maximal coefficient; 2) the larger the value of m, the larger is the value of s for the maximal coefficient of the corresponding expansion. For m=0 all four maximums correspond to $s = 0$ and the coefficients decrease symmetrically with respect to $s = 0$ in accordance to the D'Alembert rule

$$X_s^{n,m} = X_{-s}^{n,-m}. \tag{13}$$

Let us note also an interesting phenomenon in the behavior of the Hansen coefficients $L_s^{n,m}$. For $n + |m| = -1$ certain "pulsations" of the magnitude of the Hansen coefficients can be observed (see, Figures 1–2). The "pulsations" appear only in the domain of increasing the Hansen coefficients from the central minimum ($L_0^{n,m}(e) \equiv 0$ for $n + |m| = -1$). The number and the amplitude of the "pulsations" increases together with $-n$.

2.5.2. *Case* $n > 0$

The expansions with $n > 0$ are used when considering, e.g., the perturbations due to external bodies. For $n > 0$ the anomalies can be ordered according to the compactness of the corresponding expansions as follows: eccentric, elliptic, true. In this case expansion (4) in multiples of the eccentric anomaly reduces to a finite polynomial. Numerical efficiency of the expansions in multiples of the mean anomaly depends crucially on the precision to be acquired. For a low precision the series in multiples of the mean anomaly converge faster than the other ones. Because of a very fast decrease of the Hansen coefficients these series are sometimes more efficient than even the series in multiples of the eccentric anomaly which have a finite number of terms (see, for example, Figure 5 in the neighborhood of maximum). For a higher precision the efficiency of the series in multiples of the mean anomaly gets worse rapidly.

Figures 5–7 show typical behavior of $V_s^{n,m}(e)$, $G_s^{n,m}(e)$, $L_s^{n,m}(e)$, $W_s^{n,m}(e)$ for $n > 0$. Our experiments show that the series in multiples of the mean anomaly are more efficient for larger values of n. The efficiency of the series in multiples of the true anomaly decreases with increasing

of n. The coefficients $W_s^{n,m}(e)$ of the series in multiples of the elliptic anomaly do not decrease monotonically from the central maximum, but exhibit irregular pulsations of magnitudes (see, for example, Figure 5).

Let us make some notes on the behavior of Hansen coefficients. The larger the index m, the more asymmetric is the decrease of the Hansen coefficients from the central maximum. This fact is observed visually on Figure 6. On the same Figure 6 we see that Hansen coefficients exhibit again certain "pulsations" of magnitude. These "pulsations" are larger and more frequent for larger values of n and m.

For larger eccentricities all the effects described above (e.g., number and amplitude of the "pulsations" for Hansen coefficients, etc.) are amplified. Numerical efficiency of all the expansions under consideration decreases with increasing the eccentricity. The described advantages and disadvantages of the anomalies for highly eccentric orbits are also amplified. On the opposite, for smaller eccentricities the differences in the behavior of $V_s^{n,m}(e)$, $G_s^{n,m}(e)$, $L_s^{n,m}(e)$, $W_s^{n,m}(e)$ become smaller and the numerical efficiency of all four kinds of expansions is almost the same.

The results of our investigations are described in more detail in (Vasiliev, Vakhidov and Klioner, 1996). This work contains a large number of figures presenting the behavior of Fourier coefficients for four representative values of the eccentricity: 0.1, 0.5, 0.75, 0.9. These figures confirm visually the effects described above. The figures, numerical values of the coefficients as well as the software enabling one to compute the expansions are available from the authors upon request.

3. Derivatives of the Hansen-like Coefficients

Our approach allows one to evaluate not only the coefficients $V_s^{n,m}(e)$, $G_s^{n,m}(e)$, $L_s^{n,m}(e)$, $W_s^{n,m}(e)$ but also their derivatives with respect to the eccentricity. It is very important because when constructing analytical and semi-analytical theories of motion we need to integrate differential equations (for example, Lagrange equations or canonical equations for Delaunay variables) containing in the right-hand sides the derivatives of the perturbing function with respect to the orbital elements, rather than the perturbing function itself. We describe below how to solve this problem in the framework of our approach.

3.1. True Anomaly

We consider the left-hand side of (3) as a function of e and v

$$F_v\,(e,v) = \left(1-e^2\right)^n \frac{\exp\left(\overset{\circ}{\imath}\, mv\right)}{(1+e\cos v)^n}\,. \tag{14}$$

Differentiating this relation with respect to e we get

$$\frac{\partial F_v}{\partial e} = A_v\, F_v, \quad A_v = -n\left(\frac{2e}{1-e^2} + \frac{\cos v}{1+e\cos v}\right). \tag{15}$$

On the other hand, we see that

$$\frac{\partial F_v}{\partial e} = \sum_{s=-\infty}^{\infty} \frac{dV_s^{n,m}\,(e)}{de} \exp\left(\overset{\circ}{\imath}\, sv\right). \tag{16}$$

Therefore, the Fourier coefficients of the function A_vF_v coincide with the derivatives $dV_s^{n,m}\,(e)\,/de$ we are looking for. In order to compute the Fourier expansion of A_vF_v our approach described in Section 2 can be applied identically.

The similar way can be used also for computing derivatives of the coefficients $G_s^{n,m}(e)$, $L_s^{n,m}(e)$ and $W_s^{n,m}(e)$.

3.2. Eccentric Anomaly

We consider the left-hand side of (4) as a function of e and g

$$F_g\,(e,g) = \left(1-e^2\right)^n \frac{\exp\left(\overset{\circ}{\imath}\, mv(e,g)\right)}{(1+e\cos v(e,g))^n}\,. \tag{17}$$

Here v is considered as a function of e and g

$$\cos v = \frac{\cos g - e}{1-e\cos g}\,, \qquad \sin v = \frac{\sqrt{1-e^2}\sin g}{1-e\cos g}\,. \tag{18}$$

Using the equation

$$\frac{\partial v\,(e,g)}{\partial e} = \frac{\sin v}{1-e^2}\,, \tag{19}$$

one gets

$$\frac{\partial F_g}{\partial e} = A_g\; F_g\,, \quad A_g = \frac{1}{1-e^2}\left(-n\,(\cos v + e) + \overset{\circ}{\imath}\, m\sin v\right). \tag{20}$$

3.3. Mean Anomaly

The left-hand side of (6) can considered as a function of e and l

$$F_l\left(e,l\right)=\left(1-e^2\right)^n\frac{\exp\left(\overset{\circ}{\imath}\, mv(e,l)\right)}{\left(1+e\cos v(e,l)\right)^n}\,, \tag{21}$$

where v is considered here as a function of e and l. Taking the derivative of (7) one gets

$$\frac{\partial g\left(e,l\right)}{\partial e}=\frac{\sin v}{\sqrt{1-e^2}}\,, \tag{22}$$

$$\frac{\partial v\left(e,l\right)}{\partial e}=\frac{\sin v}{1-e^2}\left(2+e\cos v\right)\,. \tag{23}$$

and, therefore,

$$\frac{\partial F_l}{\partial e}=A_l\ F_l\,,$$

$$A_l=\frac{1}{1-e^2}\left(-n\cos v\left(1+e\cos v\right)+\overset{\circ}{\imath}\, m\sin v\left(2+e\cos v\right)\right)\,. \tag{24}$$

3.4. Elliptic Anomaly

The left-hand side of (9) can be considered as a function of e and w

$$F_w\left(e,w\right)=\left(1-e^2\right)^n\frac{\exp\left(\overset{\circ}{\imath}\, mv(e,w)\right)}{\left(1+e\cos v(e,w)\right)^n}\,. \tag{25}$$

Here v is considered as a function of e and w. Hence we get

$$\frac{\partial F_w}{\partial e}=A_w\ F_w\,,$$

$$A_w=n\frac{-2e-e^2\cos v-\cos v}{\left(1+e\cos v\right)\left(1-e^2\right)}+\left(\frac{en\sin v}{1+e\cos v}+\overset{\circ}{\imath}\, m\right)\frac{\partial v\left(e,w\right)}{\partial e}\,. \tag{26}$$

In order to compute $\partial v\left(e,w\right)/\partial e$ we differentiate one of the relations (18) taking into account that g is considered as a function of e and w here. The result is

$$\frac{\partial v\left(e,w\right)}{\partial e}=\frac{\sin v}{1-e^2}+\frac{1+e\cos v}{\sqrt{1-e^2}}\ \frac{\partial g\left(e,w\right)}{\partial e}\,. \tag{27}$$

There are many ways to compute $\partial g\left(e,w\right)/\partial e$. We could, for example, differentiate the series (11) with respect to e (the nome q depends only on the eccentricity e). Alternatively we could differentiate in closed

form the definition (10). Here we prefer another way, which avoids both expansions and the use of the elliptic amplitide $\mathrm{am}(x,e)$. Considering (8) as an implicit function for $g(e,w)$ we get

$$\begin{aligned}
\frac{\partial g\,(e,w)}{\partial e} &= -\left(\frac{\partial w\,(e,g)}{\partial g}\right)^{-1}\frac{\partial w\,(e,g)}{\partial e}\,,\\
\frac{\partial w\,(e,g)}{\partial e} &= \frac{\pi}{2(K\,(e))^2}\left[\frac{\partial F\,(g+\frac{\pi}{2},e)}{\partial e}K\,(e)-F\left(g+\frac{\pi}{2},e\right)\frac{dK\,(e)}{de}\right]\,,\\
\frac{\partial w\,(e,g)}{\partial g} &= \frac{\pi}{2K\,(e)}\frac{\partial F\,(g+\frac{\pi}{2},e)}{\partial g}\,,
\end{aligned} \tag{28}$$

and the derivatives of the elliptic integrals are defined as

$$\frac{\partial F\,(\alpha,e)}{\partial e} = \frac{1}{1-e^2}\left[\frac{E\,(\alpha,e)-(1-e^2)\,F\,(\alpha,e)}{e}-\frac{e\sin\alpha\cos\alpha}{\sqrt{1-e^2\sin^2\alpha}}\right]\,, \tag{29}$$

$$\frac{\partial F\,(\alpha,e)}{\partial \alpha} = \frac{1}{\sqrt{1-e^2\sin^2\alpha}}\,, \tag{30}$$

$$\frac{dK\,(e)}{de} = \frac{E\,(e)-(1-e^2)\,K\,(e)}{(1-e^2)\,e}\,. \tag{31}$$

Here $E\,(\alpha,e)$ and $E\,(e)$ are the incomplete and complete elliptic integrals of the second kind, respectively.

3.5. Numerical Results

In order to investigate the efficiency of trigonometric series with the coefficients $dV_s^{n,m}\,(e)\,/de$, $dG_s^{n,m}\,(e)\,/de$, $dL_s^{n,m}\,(e)\,/de$, $dW_s^{n,m}\,(e)\,/de$ we have computed the series numerically for various eccentricities and for various values of n and m. We used herewith the software described in Section 3 generalized in an obvious way to cope with the functions (15), (20), (24) and (26).

The results can be summarized as follows. For each anomaly the behavior of derivatives of the Fourier coefficients is quite similar to the behavior of the Fourier coefficients themselves as far as the efficiency of the corresponding expansions is concerned. Numerical values of the derivatives are usually larger than the values of the coefficients themselves. On Figures 8–10 one can see some examples of typical behavior of the derivatives. A large number of figures for the derivatives can be found in (Vasiliev *et al.*, 1997). Additional figures, numerical values of the derivatives as well as the corresponding software are available from the authors upon request.

3.6. Higher-Order Derivatives

Computation of the higher-order derivatives of $V_s^{n,m}(e)$, $G_s^{n,m}(e)$, $L_s^{n,m}(e)$, $W_s^{n,m}(e)$ (which are necessary for constructing of higher-order theories of motion) can be realized in essentially the same way as that of the first-order derivatives. Indeed, let us consider the left-hand side of (1) as a function of e and an arbitrary anomaly x

$$F_x\,(e,x) = \left(1-e^2\right)^n \frac{\exp\left(\overset{\circ}{\imath}\, mv(e,x)\right)}{(1+e\cos v(e,x))^n}\,, \tag{32}$$

where v is considered as a function of e and x. Using the approach described above we obtain quite generally

$$\frac{\partial F_x}{\partial e} = A_x\ F_x\,. \tag{33}$$

One more differentiation gives

$$\frac{\partial^2 F_x}{\partial e^2} = \left(\frac{\partial A_x}{\partial e} + (A_x)^2\right)\ F_x\,. \tag{34}$$

On the other hand,

$$\frac{\partial^2 F_x}{\partial e^2} = \sum_{s=-\infty}^{\infty} \frac{d^2 X_s^{n,m}\,(e)}{de^2} \exp\left(\overset{\circ}{\imath}\, sx\right)\,. \tag{35}$$

Thus, the Fourier series of the right-hand side of (34) gives us the second-order derivatives $d^2 X_s^{n,m}\,(e)\,/de^2$. In the same way we could derive the "generating functions" for the derivatives of any order. Although for the higher-order derivatives the expressions are rather complicated, the derivation can be easily automated with the aid of any computer algebra system (what we in fact did even for the first-order derivatives).

4. Concluding Remarks

The approach described in the present paper enables one to evaluate by means of the fast Fourier transform not only the coefficients considered in the paper and their derivatives, but also coefficients of other Fourier expansions which are used in modern celestial mechanics. In the same way one can evaluate, for example, the Hansen-like coefficients corresponding to other anomalies, the coefficients of the generalized Kepler equation (see, Brumberg, 1992; Klioner, 1992), the functions $F\,(e)$ and $G\,(e)$ introduced in (Brumberg et al., 1995), Laplace coefficients, etc. The derivatives of the corresponding coefficients can be computed as

well. Simultaneous computation of a substantial numbers of harmonics allows one to judge how efficient the corresponding expansion is and how many terms are necessary to attain a required level of accuracy. In particular, our software enables one to calculate how many terms of an expansion we have to retain in order to represent the corresponding function of elliptic motion with a given accuracy. In principle, a similar FFT-based approach could be applied to investigate actual efficiency of various variants of analytical and semi-analytical theories of motion of artificial satellites and other celestial bodies (see, e.g., Klioner, 1997). A detailed study of the latter problem is underway.

Acknowledgements

The authors are very grateful to Dr. Alexander M. Fominov for useful discussions. S.K. kindly acknowledges the receipt of a research fellowship of the Alexander von Humboldt Foundation.

References

Bond V.R., Janin G.: 1981, Canonical orbital elements in terms of an arbitrary independent variable. *Celest. Mech.,* **23**, 159

Brumberg E.V.: 1992, Perturbed two-body motion with elliptic functions. *Proc. 25th Symp. on Celest. Mech.,* NAO, Tokyo, 139

Brumberg E.V., Brumberg V.A., Konrad Th., Soffel M.: 1995, Analytical linear perturbation theory for highly eccentric satellite orbits. *Celest. Mech. and Dynam. Astron.,* **61**, 369

Brumberg E.V., Fukushima T.: 1994, Expansions of elliptic motion based on elliptic function theory. *Celest. Mech. and Dynam. Astron.,* **60**, 69

Brumberg V.A., Klioner S.A.: 1995, Numerical efficiency of the elliptic function expansions of the first-order intermediary for general planetary theory. In: S.Ferraz-Mello, B.Morando, J.E.Arlot (eds.), *Dynamics, ephemerides and astrometry in the solar system*, Kluwer, Dordrecht, 101

Chapront J., Simon J.-L.: 1996, Planetary theories with the aid of the expansions of elliptic functions. *Celest. Mech. and Dynam. Astron.,* **63**, 171

Char B.W., Geddes K.O., Gonnet G.H., Leong B.L., Monagan M.B., Watt S.M.: 1993, MAPLE V Library Reference Manual. Springer, New York

Danby J.M.A., Burkardt T.M.: 1983, The solution of Kepler's equation, I. *Celest. Mech.,* **31**, 95

Ferrandiz J.M., Ferrer S., Sein–Echaluce M.L.: 1987, Generalized elliptic anomalies. *Celest. Mech.,* **40**, 315

Goad C.C.: 1987, An efficient algorithm for the evaluation of inclination and eccentricity functions. *Manuscripta Geodaetica*, **12**, 11

Klioner S.A.: 1992, Some typical algorithms of the perturbation theory within *Mathematica* and their analysis. *Proc. 25th Symp. on Celest. Mech.,* NAO, Tokyo, 172

Klioner S.A.: 1997, On the Expansions of Intermediate Orbit for General Planetary Theory. *Celest. Mech. and Dynam. Astron., in press*

Klioner S.A., Vakhidov A.A., Vasiliev N.N.: 1996, Fast Fourier transform for studying the convergence of elliptic motion series. *Proc. of International Workshop "New computer technologies in control systems",* Pereslavl-Zalessky, 34

Press W.H., Teukolsky S.A., Vetterling W.T., Flannery B.P., 1992. Numerical Recipes In Fortran: the art of scientific computing. Cambridge University Press, New York

Vakhidov A.A., Vasiliev N.N.: 1996, Development of analytical theory of motion for satellites with large eccentricities. *Astron. Journ.,* **112**, 2330

Vasiliev N.N., Vakhidov A.A., Klioner S.A.: 1996, On the convergence of elliptic motion series with different trigonometric arguments. *ITA RAS Preprint,* No 60

Vasiliev N.N., Vakhidov A.A., Klioner S.A.: 1997, Numerical computation of derivatives of Hansen–like coefficients by means of the fast Fourier transform. *ITA RAS Preprint, in press*

Vasiliev N.N., Vakhidov A.A., Sokolsky A.G.: 1996, Analytical theory of perturbations of the first order in motion of a highly elliptic artificial Earth satellite. *ITA RAS Preprint,* No 55

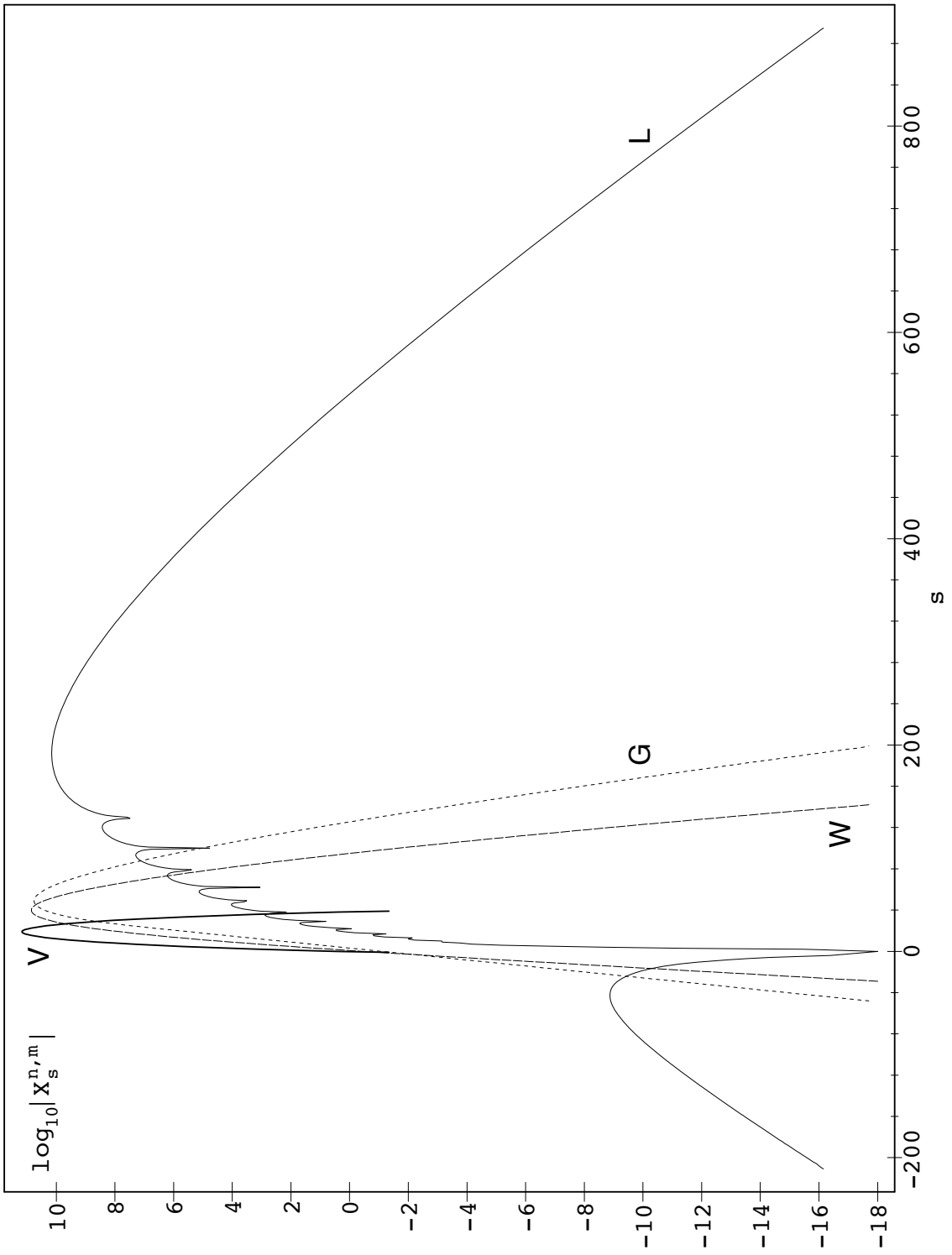

Figure 1. The behavior of $|V_s^{n,m}(e)|$ $(s \in [-1, 39])$, $|G_s^{n,m}(e)|$ $(s \in [-48, 199])$, $|L_s^{n,m}(e)|$ $(s \in [-211, 895])$, $|W_s^{n,m}(e)|$ $(s \in [-29, 142])$ for $e = 0.75$, $n = -20$, $m = 19$. Note that the series (3) reduce to a polynomial for $n < 0$. Therefore, there exists only a finite number of $V_s^{n,m}(e)$ in this case and all of them are shown on all Figures corresponding to $n < 0$. We intensionally show the behavior of the coefficients for rather large values of $|n|$ and $|m|$ to make the behavior more clearly visible on the plots. To produce the coefficients presented on all Figures of this paper we used 32 decimal digits arithmetic as implemented in Maple.

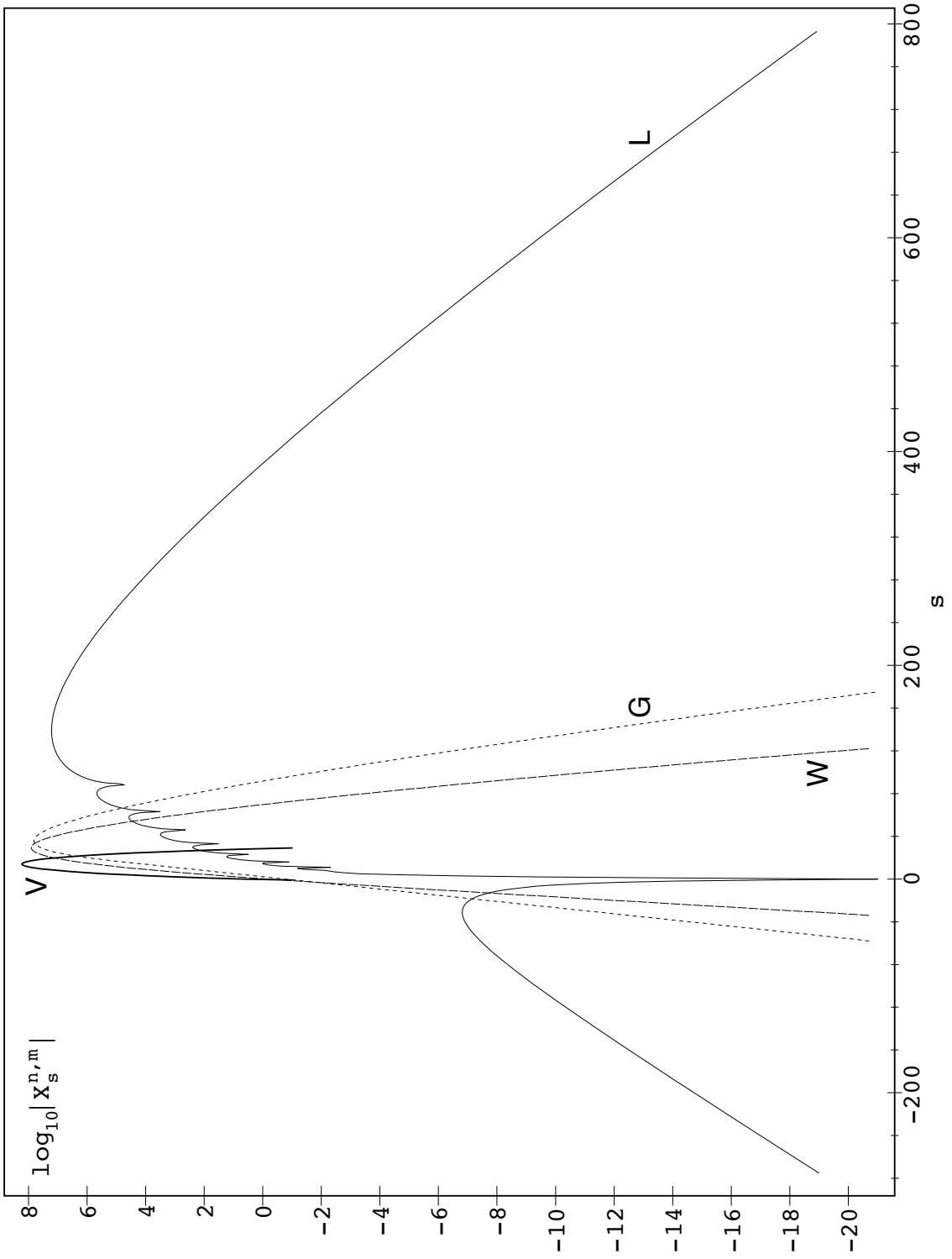

Figure 2. The behavior of $|V_s^{n,m}(e)|$ ($s \in [-1, 29]$), $|G_s^{n,m}(e)|$ ($s \in [-58, 175]$), $|L_s^{n,m}(e)|$ ($s \in [-275, 793]$), $|W_s^{n,m}(e)|$ ($s \in [-34, 122]$) for $e = 0.75$, $n = -15$, $m = 14$.

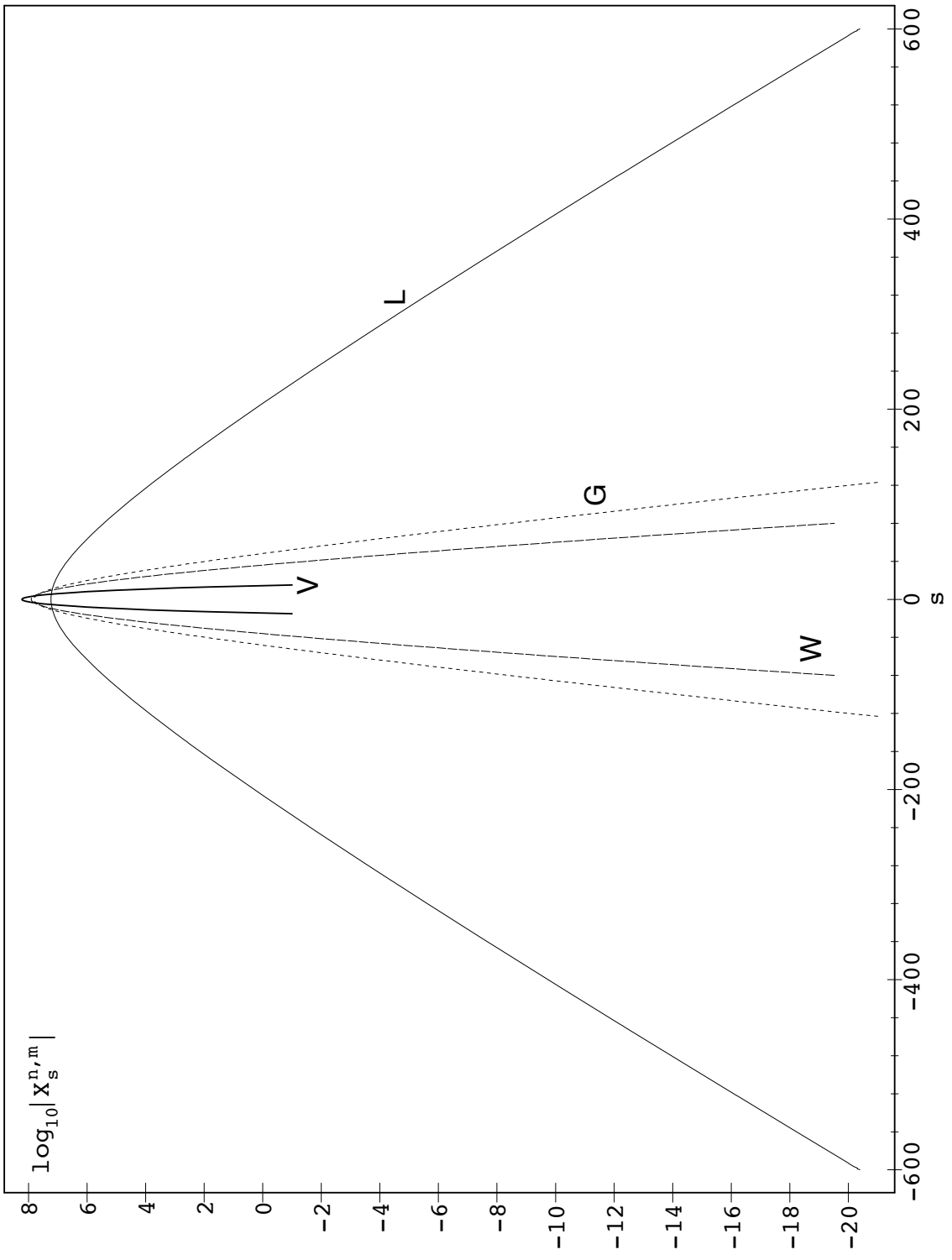

Figure 3. The behavior of $|V_s^{n,m}(e)|$ ($s \in [-15, 15]$), $|G_s^{n,m}(e)|$ ($s \in [-123, 123]$), $|L_s^{n,m}(e)|$ ($s \in [-600, 600]$), $|W_s^{n,m}(e)|$ ($s \in [-80, 80]$) for $e = 0.75$, $n = -15$, $m = 0$.

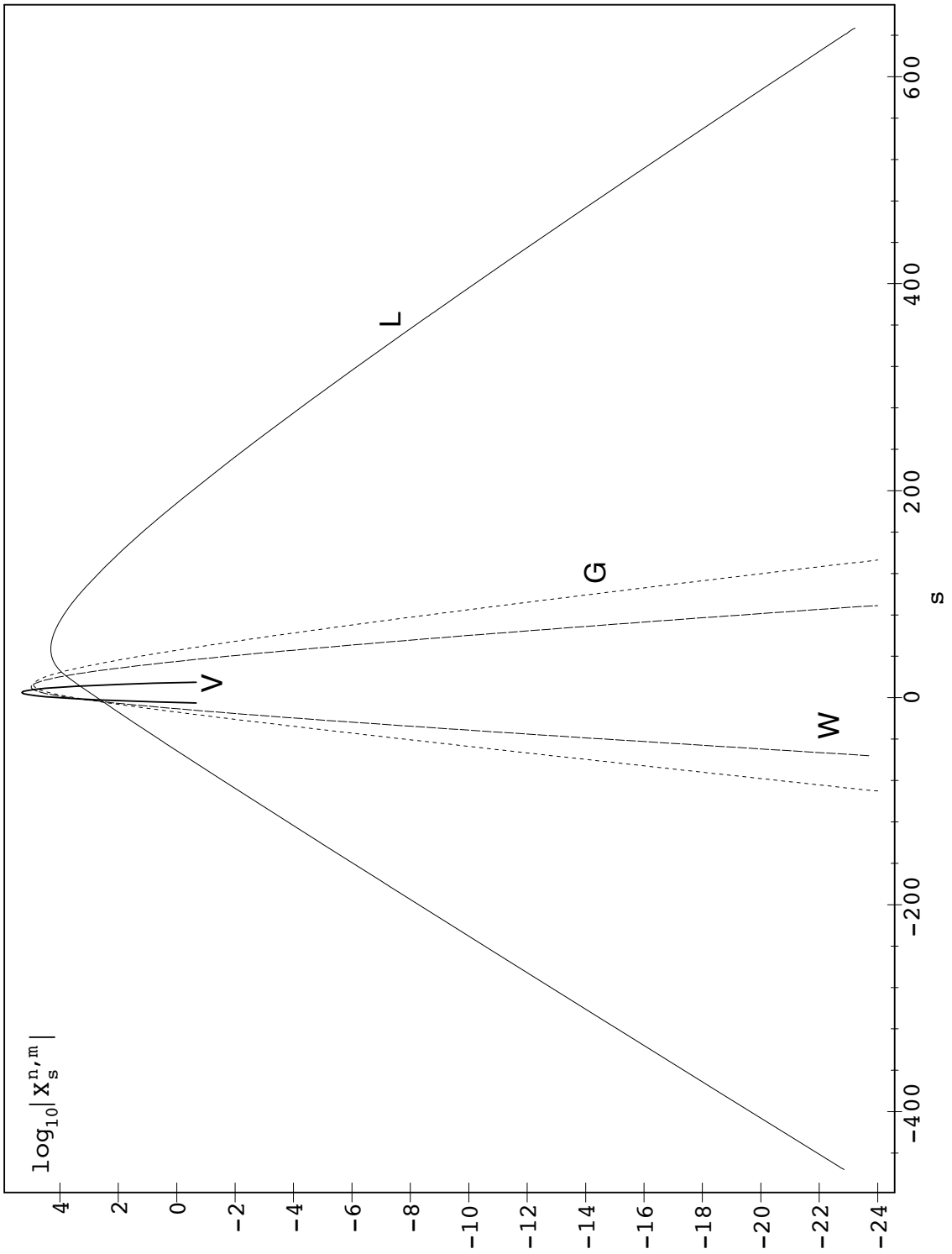

Figure 4. The behavior of $|V_s^{n,m}(e)|$ ($s \in [-5, 15]$), $|G_s^{n,m}(e)|$ ($s \in [-90, 133]$), $|L_s^{n,m}(e)|$ ($s \in [-456, 647]$), $|W_s^{n,m}(e)|$ ($s \in [-56, 89]$) for $e = 0.75$, $n = -10$, $m = 5$.

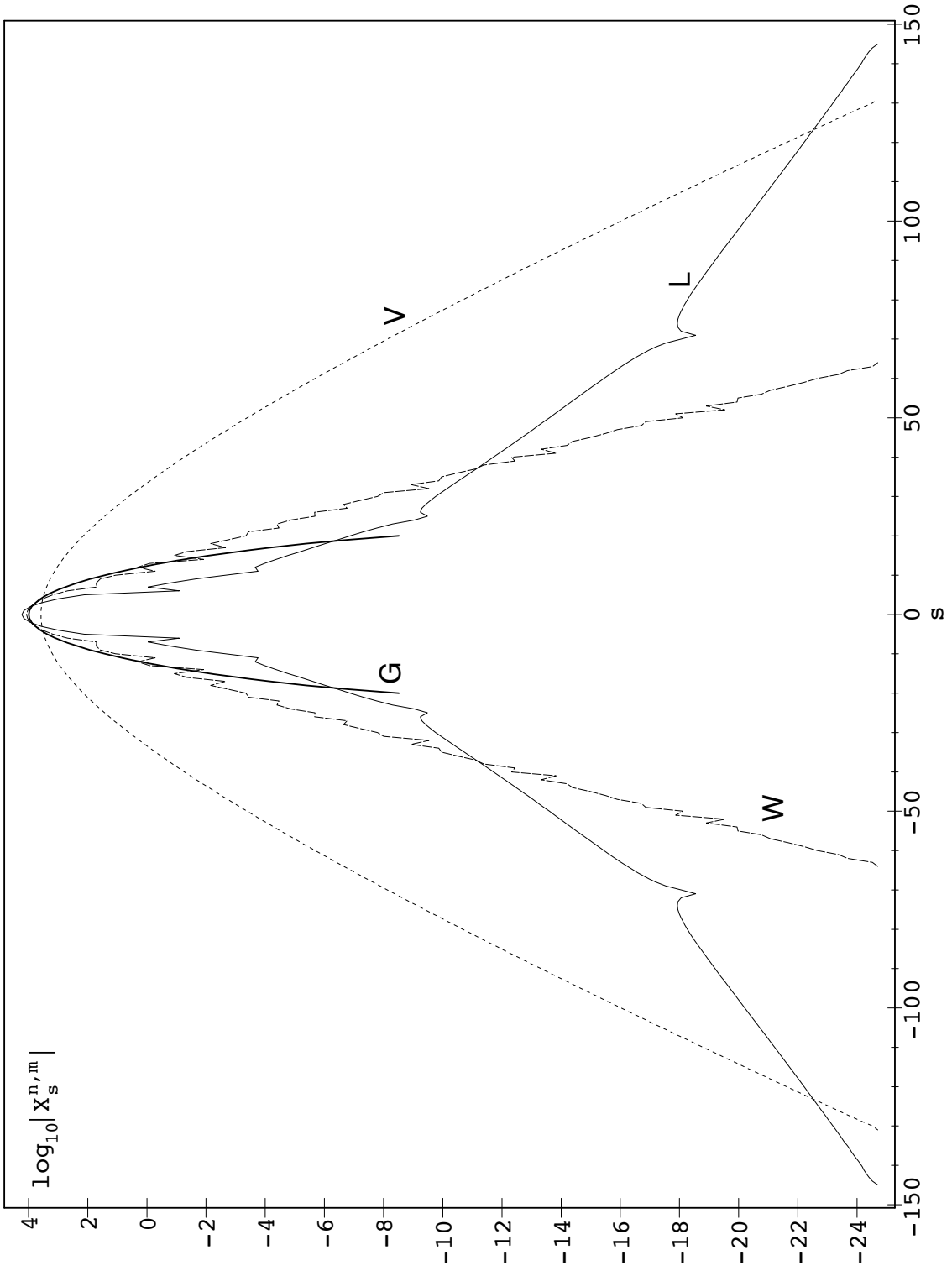

Figure 5. The behavior of $|V_s^{n,m}(e)|$ ($s \in [-131, 131]$), $|G_s^{n,m}(e)|$ ($s \in [-20, 20]$), $|L_s^{n,m}(e)|$ ($s \in [-145, 145]$), $|W_s^{n,m}(e)|$ ($s \in [-64, 64]$) for $e = 0.75$, $n = 20$, $m = 0$. Note that the series (4) reduce to a polynomial for $n > 0$. Therefore, there exists only a finite number of $G_s^{n,m}(e)$ in this case and all of them are shown on all Figures corresponding to $n > 0$.

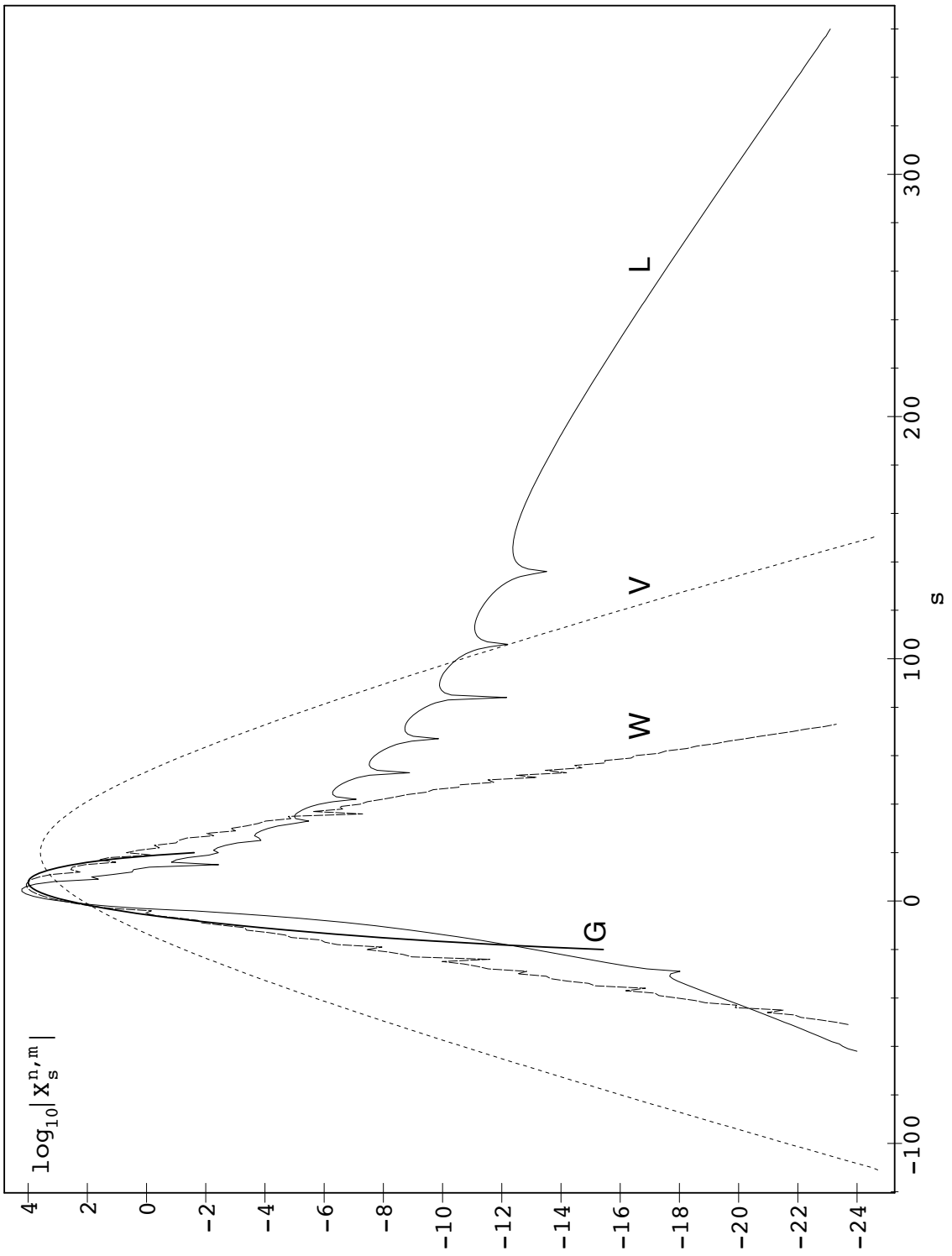

Figure 6. The behavior of $|V_s^{n,m}(e)|$ ($s \in [-111, 151]$), $|G_s^{n,m}(e)|$ ($s \in [-20, 20]$), $|L_s^{n,m}(e)|$ ($s \in [-62, 360]$), $|W_s^{n,m}(e)|$ ($s \in [-51, 73]$) for $e = 0.75$, $n = 20$, $m = 20$.

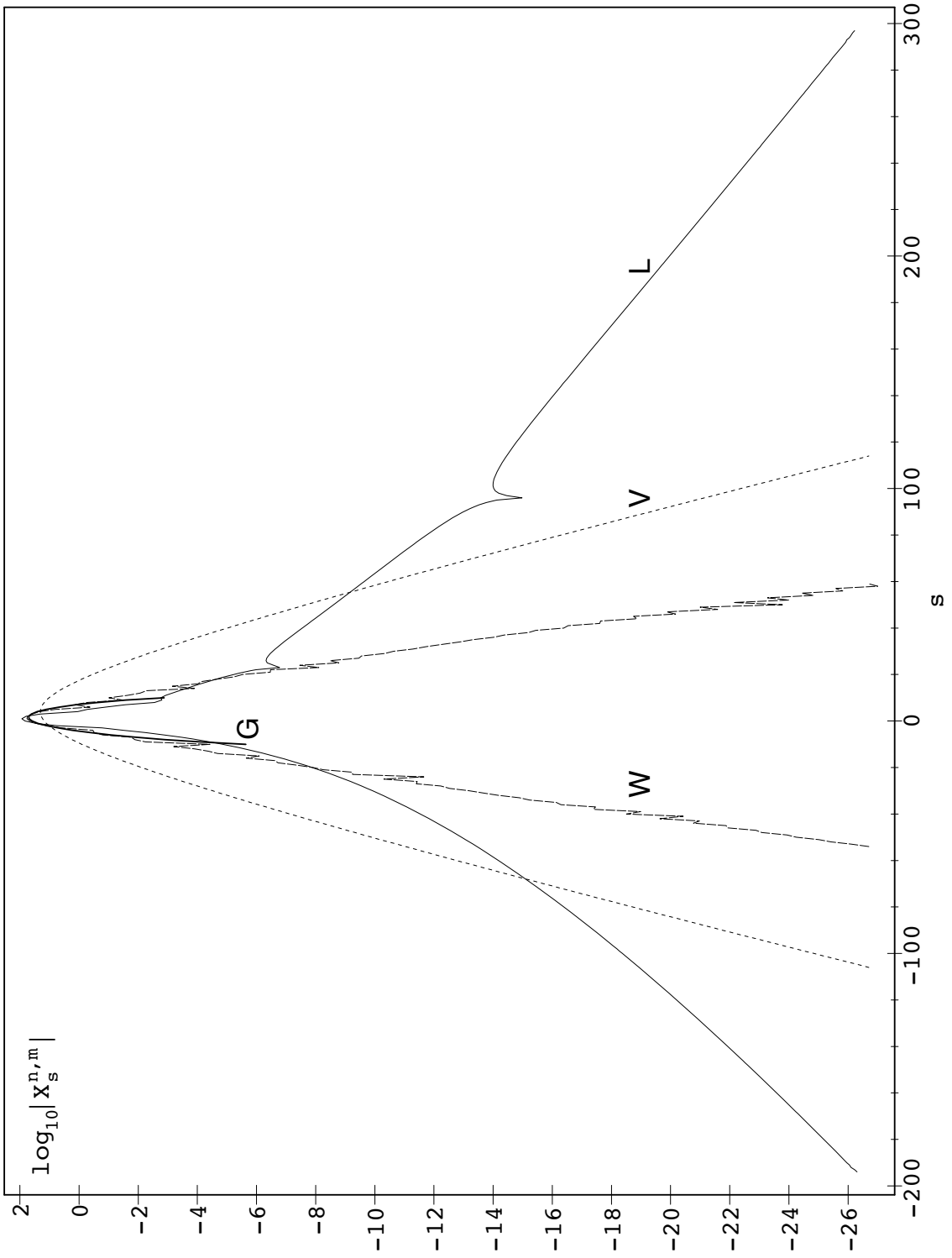

Figure 7. The behavior of $|V_s^{n,m}(e)|$ $(s \in [-106, 114])$, $|G_s^{n,m}(e)|$ $(s \in [-10, 10])$, $|L_s^{n,m}(e)|$ $(s \in [-194, 297])$, $|W_s^{n,m}(e)|$ $(s \in [-54, 59])$ for $e = 0.75$, $n = 10$, $m = 4$.

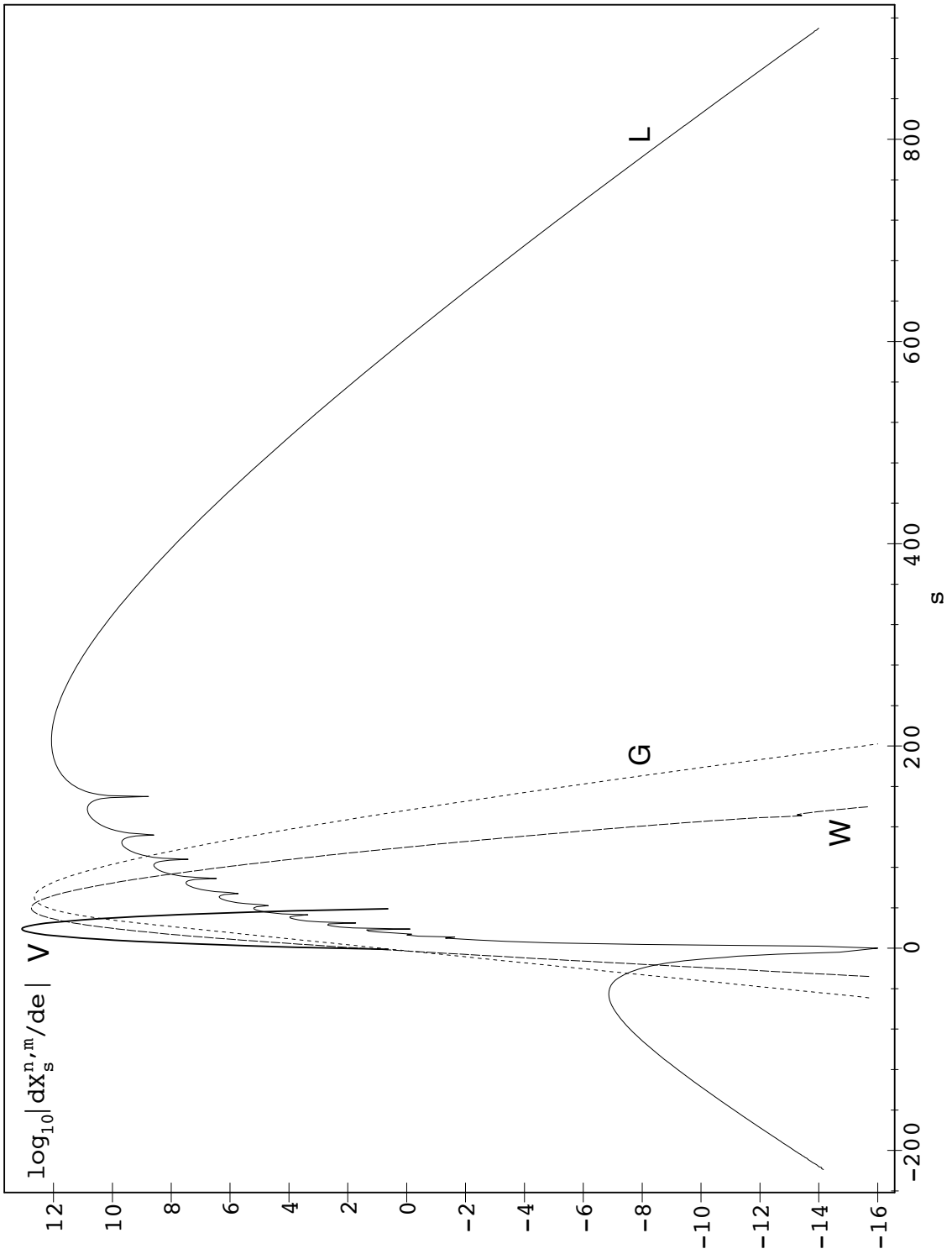

Figure 8. The behavior of $|dV_s^{n,m}(e)/de|$ ($s \in [-1, 39]$), $|dG_s^{n,m}(e)/de|$ ($s \in [-49, 202]$), $|dL_s^{n,m}(e)/de|$ ($s \in [-219, 910]$), $|dW_s^{n,m}(e)/de|$ ($s \in [-28, 140]$) for $e = 0.75$, $n = -20$, $m = 19$.

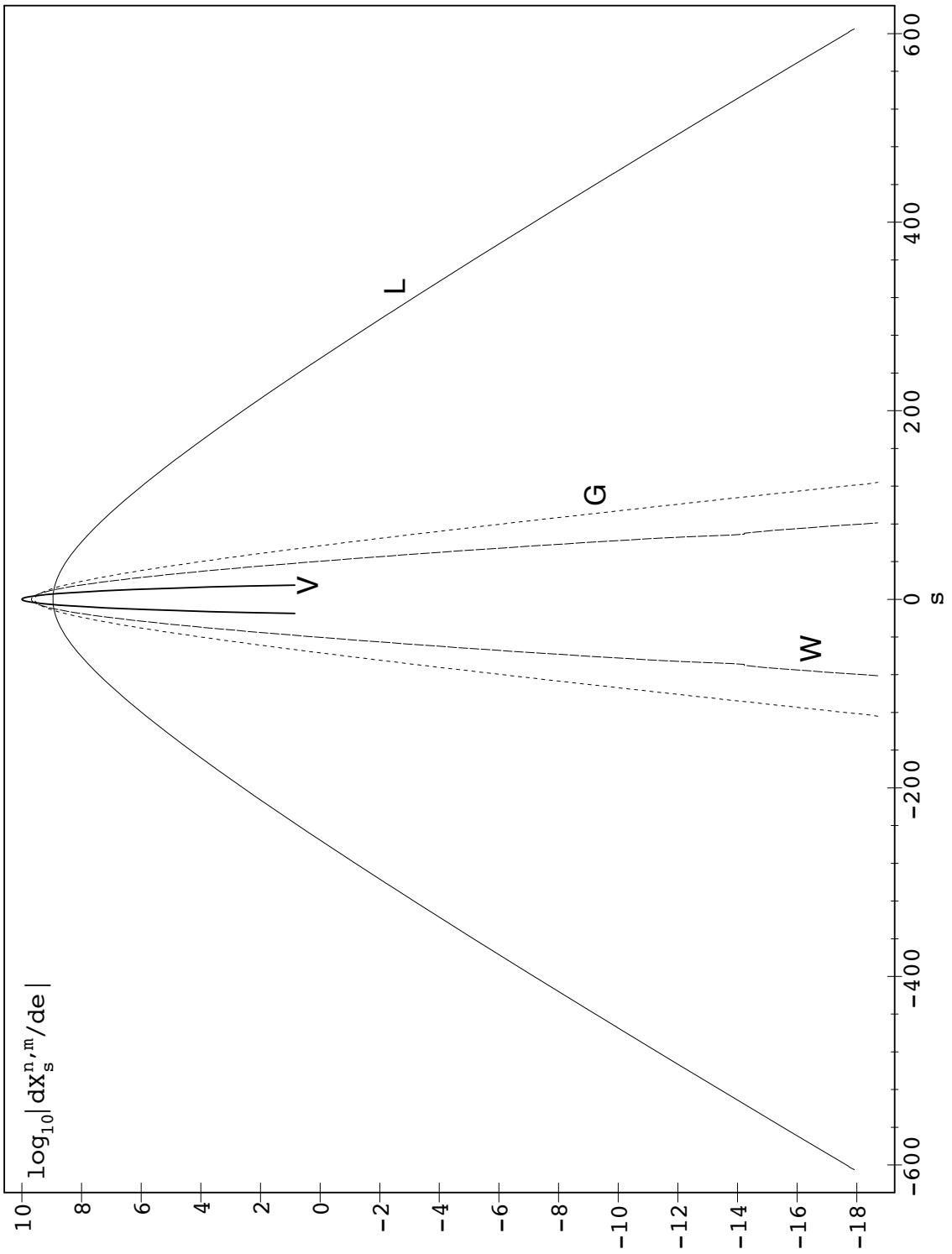

Figure 9. The behavior of $|dV_s^{n,m}(e)/de|$ ($s \in [-15, 15]$), $|dG_s^{n,m}(e)/de|$ ($s \in [-124, 124]$), $|dL_s^{n,m}(e)/de|$ ($s \in [-605, 605]$), $|dW_s^{n,m}(e)/de|$ ($s \in [-81, 81]$) for $e = 0.75$, $n = -15$, $m = 0$.

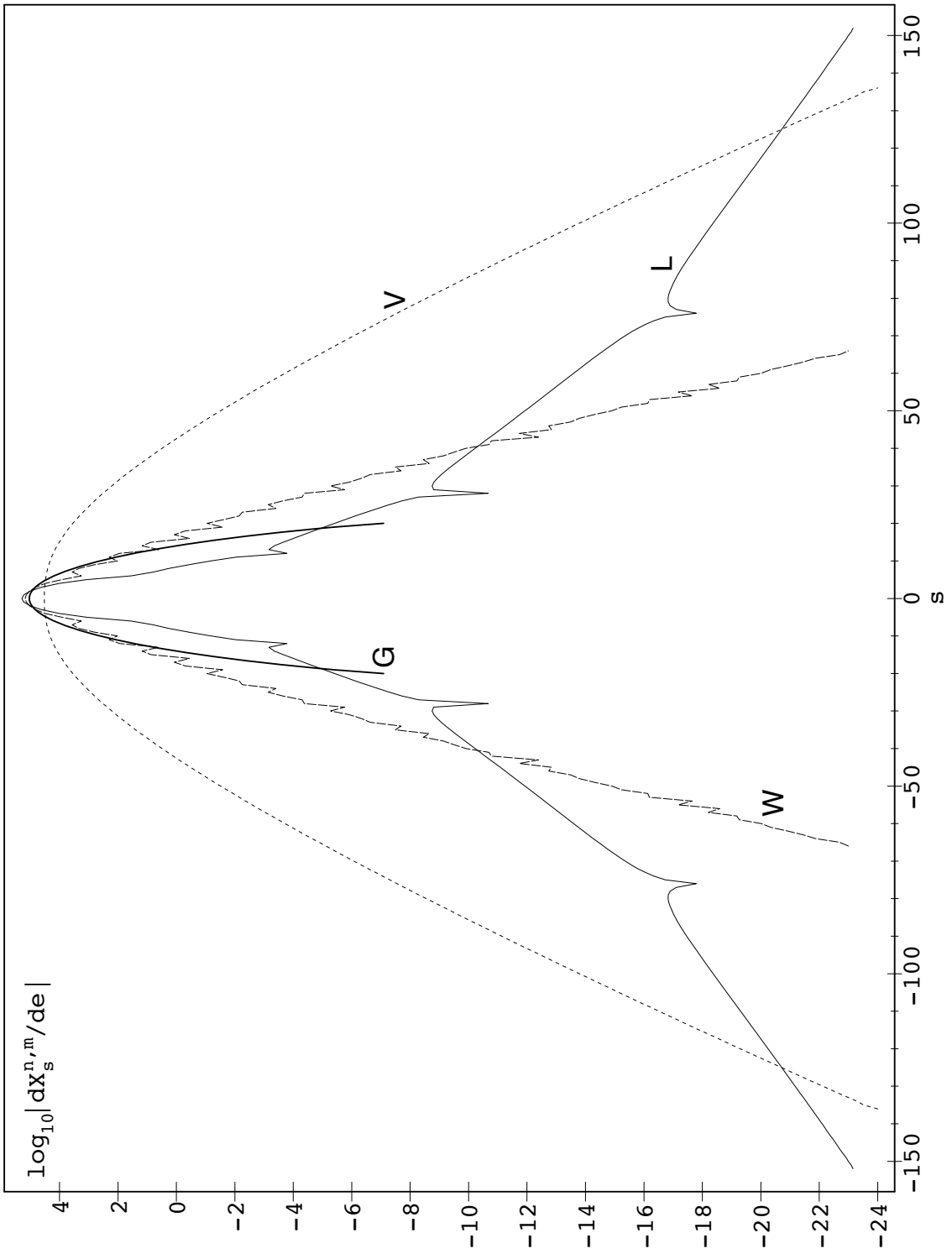

Figure 10. The behavior of $|dV_s^{n,m}(e)/de|$ ($s \in [-136, 136]$), $|dG_s^{n,m}(e)/de|$ ($s \in [-20, 20]$), $|dL_s^{n,m}(e)/de|$ ($s \in [-152, 152]$), $|dW_s^{n,m}(e)/de|$ ($s \in [-66, 66]$) for $e = 0.75$, $n = 20$, $m = 0$.